



OPEN

Colorful and facile in situ nanosilver coating on sisal/cotton interwoven fabrics mediated from European larch heartwood

K. M. Faridul Hasan^{1✉}, Péter György Horváth¹, Zsófia Kóczán², Miklós Bak¹ & Tibor Alpar^{1✉}

This study reports on a novel coloration approach for sisal/cotton interwoven fabric via in situ synthesis of European larch (*Larix decidua*) heartwood-anchored sustainable nanosilver. The heartwood extracts functioned as the reducing and stabilizing agent in reaction systems. The deposited silver nanoparticles (AgNPs) over the fabric surfaces displayed brilliant coloration effects with improved fastness ratings and color strengths (K/S). The successful depositions of nanosilvers were quantified and increasing trends in K/S values with the increase in silver precursor loading were discovered. The concentrations of AgNPs deposited on fabric surfaces were found to be 16 mg/L, 323 mg/L, and 697 mg/L, which were measured through an ICP OES (atomic absorption spectroscopy) test. The K/S values obtained for different loadings of silver precursors (0.5, 1.5, and 2.5 mM (w/v)) are 2.74, 6.76, and 8.96. Morphological studies of the control and AgNP-treated fabrics also displayed a uniform and homogeneous distribution of AgNPs over the fabric surfaces. FTIR (Fourier transform infrared spectroscopy) studies of the sustainably developed materials further confirms the successful bonding between the fabrics and AgNPs. Furthermore, stability against temperature was also noticed as per TGA (thermogravimetric analysis) and DTG (derivative TG) analysis although there was a slight decline from the control sisal/cotton interwoven fabrics observed. Statistically, regression analysis and ANOVA tests were conducted to understand the significance of increased nanosilver loading on sisal/cotton interwoven fabrics. In summary, the perceived results demonstrated successful coloration and functionalization of sisal/cotton interwoven fabrics through green AgNPs, which could indicate a new milestone for industrial production units.

The functionalization of natural fibers as well as associated fabrics with various nanoparticles has garnered significant attention in both daily life and in industrial production. Among different nanoparticles^{1,2}, AgNPs is the most prominent and popular due to its optical, coloration, bacterial resistance, and thermal performances³⁻⁵. AgNPs display scattering and light absorption properties, especially in their oscillation of free electrons in the presence of incident light, which is termed LSPR (localized surface plasmon resonance). Metallic nanoparticles expose diversified colors depending on the LSPR wavelength and nanoparticles size, shape, and dielectric and inter-particle distance⁶. Even though the existence of AgNPs were not confirmed in ancient times, the technology was still employed in the stained glass windows of Western churches and in lyocrogus cup colorations^{7,8}. However, the coloration of different natural and synthetic fibers using biosynthesized AgNP is still a novel approach. Research focusing on the coloration and functionalization of natural fibers derived substrates and associated fabrics has been extensive⁹⁻¹². Some studies have emphasized the necessity of cationization of natural fibers like cotton¹³. Nevertheless, any extra processing requires additional chemicals, associated energy, and operational set up, which incurs additional production costs. Though coloration of blended fiber and interwoven fabric-based textile with advanced technologies possesses significant application potential for industrial production and consumers, research into these methods has been limited. Consequently, interwoven sisal/cotton woven fabric coloration generally occurs without pretreatments under the justification that this omission saves on utility costs during operations.

¹Simonyi Károly Faculty of Engineering, University of Sopron, Sopron, Hungary. ²Paper Research Institute, Simonyi Károly Faculty of Engineering, University of Sopron, Sopron, Hungary. ✉email: faridulwtu@outlook.com; alpar.tibor@uni-sopron.hu

Fibers	Sisal ²⁹ (wt.%)	Cotton ^{29,30} (wt.%)
Cellulose	65	85–90
Hemicellulose	12	4–5.9
Lignin	9.9	0.75
Oil and wax	2	0.6

Table 1. Chemical properties of sisal and cotton.

Sisal is a potential source of naturally derived fabric and a prospective source of multifunctional textiles. Recent studies have utilized and functionalized sisal to develop composite materials^{14,15}. However, the coloration/functionalizing of sisal using nanosilver-based materials has not been studied yet. Furthermore, several attempts to functionalize sisal fibers using different types of nanoparticles have been made^{16,17}. On the other hand, cotton—due to its superior hygroscopicity, heat retention, and softness—is the dominant natural fiber in textile industries¹⁸. As noted in Table 1, cotton consists mainly of cellulose, lignin, hemicellulose, and oil and wax. Sisal fibers display chemical characteristics that are similar to cotton because both cotton and sisal are naturally originated fibers. A great deal of research has been conducted on cotton, as it is the most widely used material in clothing. Researchers also attempted to functionalize cotton with a various nanoparticles such as ZnO, Cu, TiO₂, and SiO₂^{19–21}. However, researchers have also focused considerable efforts on AgNP to color and functionalize cotton as well^{13,22,23}. Recently, researchers have also concentrated on the green synthesis of AgNPs using different naturally derived materials such as plants, flowers, stems, and leaves^{10,24–26}. Although a variety of plants that could be used to synthesize AgNPs has been investigated, the heartwoods of European larch as a stabilizing and reducing agent of silver precursors have not been studied yet. European larch is widely grown in central European countries like Hungary. Due to its colorful and aesthetic texture, European larch wood is extensively used in various outdoor applications including rails, terraces, windows, and fences as well as in indoor applications such as furniture, flooring, and stairways²⁷. However, the heartwoods extracts of European larch can also be utilized as a reducing and stabilizing agent. The present study aims to demonstrate the immense possibilities of European larch in coloration.

Technological advancements have made comfort enhancement a driving force in fabric design. In earlier fabric production, fabrics were produced wholly from the same category of fibers, like 100% cotton or 100% polyester, for example. Later, different proportions of fibers were blended together to produce more flexible fabric blends from raw materials like 65% cotton and 35% polyester. Scientists eventually utilized production technology to produce interwoven fabrics from different categories of fibers, such as yarn to produce woven fabrics. In order to produce interwoven fabrics, it is necessary to insert warp and weft yarns of different fibers in the same fabric structure. In woven structured fabrics, lengthwise yarns are termed “warp”, while crosswise yarns are called “weft”²⁸. Therefore, interwoven engineered fabrics made of warp (sisal fibers) and weft (cotton fibers) were selected for this study. The coloration of sisal/cotton interwoven fabric is also an important wet-based technology, although dyeing is still performed using traditional dyeing protocols and technology using reactive dyes, which require extensive chemicals and dyestuffs. The usage of traditional colorants poses constant threats to the environment. As a result, there is an urgent demand to explore feasible and advanced technological processes to color interwoven cellulosic fabrics in an eco-friendly way. Moreover, interwoven fabrics made of sisal and cotton fibers for nanosilver-based coloration and functionalization has not yet been explored. The current study presents a novel method for the coloration of sisal/cotton interwoven fabrics using European larch heartwood-mediated AgNPs. This study offers the interwoven coloration industry new operational technology and sustainable coloration possibilities with significant potentiality.

Experimental

Materials. Grey-colored sisal/cotton interwoven fabrics of 220 GSM (g/m²) density with a structure of interwoven fabric with cellulosic paper mat underneath was procured from Locatelli Hungária Kft. (Hungary). Initially, fabric parts were separated from the mat via boiling at 90 °C for 15 min. In the sisal/cotton interwoven fabrics, sisal yarns were engineered in warp direction, whereas cotton yarns were in weft direction. The sisal/cotton fabric samples were then washed and dried at 100 °C for 12 min. Later, 5 g samples were measured for every single nanosilver treatment. In order to synthesize AgNP, AgNO₃ reagent was procured from Sigma Aldrich Co., St. Louis, United States. European larch heartwood (scientific name *Larix decidua*) was collected as wood logs from the University of Sopron woodworking shop.

In situ biosynthesis of green AgNPs on sisal/cotton interwoven fabrics. The heartwood logs of European larch were directly collected from the woodworking shops at the University of Sopron, Hungary. The collected heartwood logs were cut into smaller pieces with a laboratory circular saw machine (DCS570N XJ model, Pennsylvania, United States)). The wood pieces (Fig. 1) were then washed with distilled water to remove any unexpected debris and dust. This was followed by drying at 120 °C for 15 min. The heartwood pieces were then crushed with a laboratory grinder until they attained powder form to ensure easy extractions into aqueous solutions. Around 100 g of *Larix decidua* powder was mixed with 500 mL of water to secure a 20% w/v aqueous solution at boiling temperature around 100 °C for 30 min. The aqueous solution was then filtered and wood wastes were removed. Afterward, the sealed and bottled extracted solution was stored in a freezer at around 4 °C for later use. AgNO₃ and *Larix decidua* solutions of different concentrations, as tabulated in Table 2, were meas-

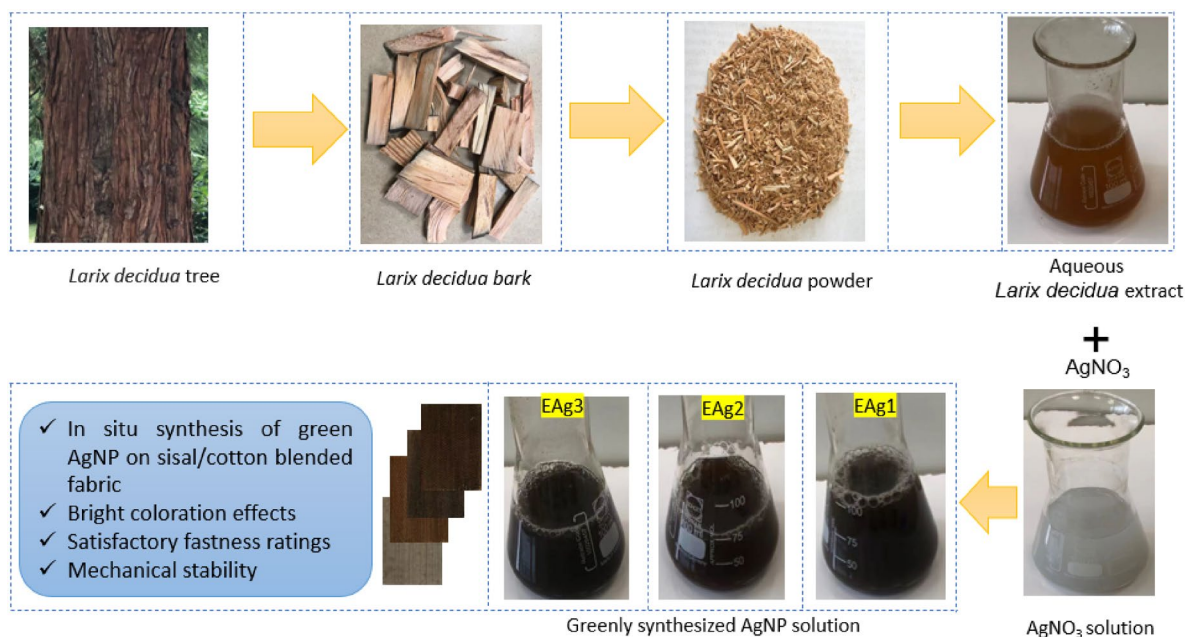


Figure 1. A schematic operational protocol for the extraction of European larch bark aqueous solution and in situ biosynthesis of nanocolloids on sisal/cotton interwoven fabrics.

Specimens	AgNO ₃ concentrations (mM)	EL (MW in % (w/v))
EAg0	0	0
EAg1	0.5	4.0
EAg2	1.5	4.0
EAg3	2.5	4.0

Table 2. Recipe protocols for control and nanosilver-coated sisal/cotton interwoven fabrics. *EL* European larch heartwood, *MW* molar weight.

ured and mixed in the beaker. The beaker was then continuously stirred until an optimal solution was prepared. The first sample, in which 0.5 mM AgNO₃ was used, was denoted as EAg1. The second (EAg2) and third sample preparation (EAg3) used 1.5 and 2.5 mM AgNO₃, respectively. The aqueous solutions of *Larix decidua* were used in 4.0 MW in % (v/v) in all cases. Both AgNO₃ and *Larix decidua* aqueous solutions were then mixed properly with a magnetic stirrer. The sisal/cotton interwoven fabrics were then immersed in the solutions and stirred for another 10 min. The color of the solutions started to change from a milky appearance to a colored state reflecting the development of a nanosilver environment in the beaker. The successful attachment of the colorful nanosilver on fabric surfaces were performed at 95 °C for 35 min. Figure 2 illustrates the detailed operational mechanism. Finally, the beakers were cooled and the samples were washed with distilled water three times at room temperature (25 °C) to remove any poorly adhered nano seeds from fabric surfaces. The samples were then subsequently dried in a laboratory dryer at 120 °C for 12 min.

Characterizations of deposited AgNPs on sisal/cotton interwoven fabrics. The moisture contents of the heartwoods and nanotreated fabrics were investigated using a moisture analyzer (Kern ULB 50–3 N model instruments, KERN AND SOHN GmbH company, Germany). Initially, the Ag contents on aqueous solutions were measured using atomic absorption spectroscopy, ICP OES, iCAP™ 6300 series, Thermo scientific, USA. The morphological observations of the control and AgNP-treated fabrics were conducted using an SEM (scanning electron microscopy) machine (SEM, S 3400 N Hitachi model, manufactured in Tokyo, Japan) at 8.00 kV. Moreover, special software (Quantax Esprit 1.9, Berlin, Germany) was used to assess the elemental compositions (EDX) and mapping. The perceived color values were measured using Konica Minolta spectrophotometer (model: CM-2600d, Japan) within 400 to 700 nm wavelengths ranged under D65 observer (standard). The chemical bonding structures of control and nanosilver treated materials were tested in terms of FTIR spectroscopy analysis within 4000 to 400 cm⁻¹ wavenumber. Thermal properties were evaluated with a Themys thermal analyzer, Setaram Instrumentation, France in terms of TGA and DTG under nitrogen atmosphere at 10 °C/min temperature gradient ranged from 10 to 800 °C. The fastness properties of the colored products were also investigated further; whereas wash fastness properties were assessed using ISO 105C06:1994 standard and rubbing fastness properties by ISO 105–X12:2003 methods by a crock meter. Standard laboratory environment

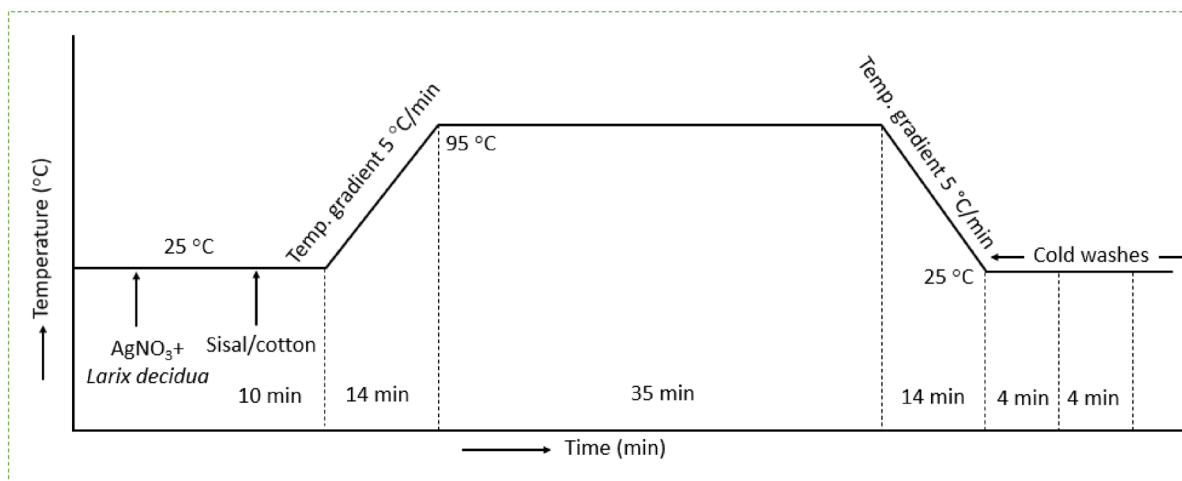


Figure 2. Operational procedures of green AgNPs deposition mechanism on sisal/cotton interwoven fabrics.

was considered for the testing ($65 \pm 5\%$ relative humidity and 20 ± 5 °C) for temperatures. Finally, grey scale was implemented to assess the ratings according to the respective tests in terms of shade changes in the clothes.

Ethical approval. This research study involved no human participants or any animal experiments. The European larch (*Larix decidua*) heartwood used in this research is complied with local institutional, national, and international guidelines and legislation. The necessary permissions for the used plant is also taken from respective authorities.

Results and discussions

In situ synthesis mechanism of AgNPs on sisal/cotton interwoven fabrics. Nanosilvers were in situ synthesized over sisal/cotton interwoven fabrics by utilizing *Larix decidua* aqueous solutions as the green capping and reducing agent for AgNO_3 . When the *Larix decidua* aqueous solutions (4.0%, v/v) were dropped in the beakers containing AgNO_3 , the color of the solutions started to change visually from a milky state to a yellowish brown. After several minutes of mixing, the color turned completely dark brown, demonstrating a successful formation of metallic AgNPs. The Ag^+ is reduced to metallic (Ag^0) after a good mixing of a silver precursor and *Larix decidua* aqueous solution, especially for the photocatalytic actions³¹. Another researcher presented a similar report³². Moreover, the color changes also occurred for the oscillation of conduction electrons in metallic nanoparticles due to LSPR properties of AgNPs. Furthermore, the color intensity depends on increased concentrations of used silver precursor in the synthesis system.

Quantification of control and AgNP treated sisal/cotton interwoven fabrics. The nanosilvers present on aqueous solutions were investigated with an iCP OES test. AgNPs present on nanocolloid for 0.5, 1.5, and 2.5 mM AgNO_3 (Table 2) precursors were 16, 323, and 697 mg/L, respectively (Fig. 3). Furthermore, AgNP contents increased with the increase of AgNO_3 in the nanocolloid environments. Similar findings were also reported in our recently published works on nanosilvers mediated from *Fraxinus excelsior* tree flowers⁴. Therefore, it could be concluded that the presence of AgNPs could be tuned and regulated by controlling the silver precursor in the reaction systems.

Morphological, EDX spectra, and elemental observations of control and AgNPs deposited on sisal/cotton interwoven fabrics. The morphological observations clearly demonstrated the presence of AgNPs on sisal/cotton interwoven fabrics (Fig. 4). A strong binding was created between the nanosilver and fabrics, which enabled the excellent interactions between them. All the fabric samples heavily displayed the presence of AgNPs, whereas control samples did not show any AgNP presence, only plain and uniform surfaces. The coated and deposited nanoparticles were also evident at the surfaces and inter-fiber spaces of the fabrics. Furthermore, the nanotreated samples also displayed a size and shape that is typical of the metallic AgNP³³.

The presence of metallic AgNPs was also confirmed by SEM-deployed EDX analysis (Fig. 5). All the nanoparticle coated samples exhibited a typical peak at around 2.96 keV, which was absent from the control sample³⁴. Moreover, in addition to the presence of C and O (typical chemical elements of cellulosic materials and metabolites present in plants) in all the samples, Cl was also present. This may have been due to the presence of plant-derived materials. In addition, all plants inherently possess ample nutrients like chloride ions^{34,35}. Other impurities like S, Si, and Ca were observed in small amounts, attesting to the possibility that these may have been generated during processing. The wt% of C and O did not vary significantly within the nanosilver treated fabrics but it did vary within the control (50.08 and 47.94%, respectively) and other samples (41.37, 45.6, and 43.39% C and 44.1, 43.3, and 43.1% O, respectively for samples 2, 3, and 4). Furthermore, there was a slight difference in wt% between 0.5 and 1.5 mM silver precursor treated samples where the values were 9.462% and 9.463%,

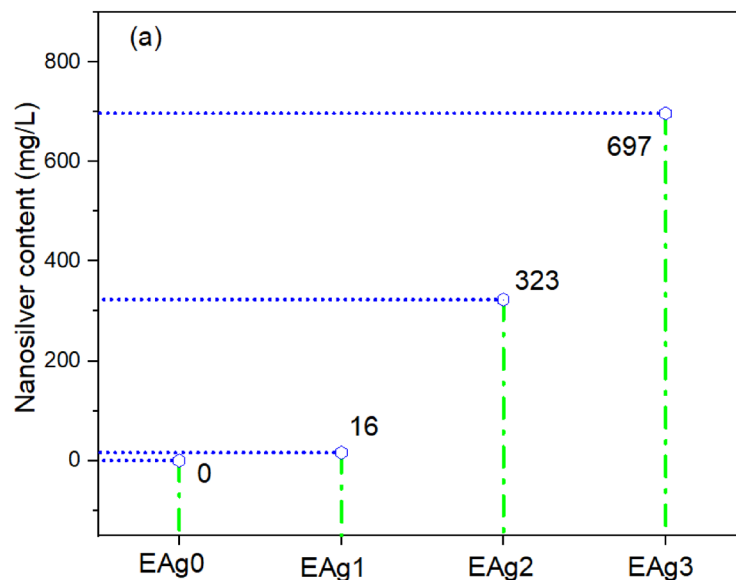


Figure 3. iCP OES test analysis for nanocolloids developed over sisal/cotton interwoven fabrics.

respectively (Table 3). However, the wt% of sample 4 revealed significant differences in nanosilver contents (9.95%), which was around 5.15% higher than in samples 2 and 3. A similar detection of chemical elements (C and O for the control sample and Ag for the nanocoated samples) in the control and nanosilver treated fabrics was also observed in elemental mapping analysis. A homogeneous and uniform distribution of C, O, and Ag was also explicitly observed in the overlapping images (Fig. 6) demonstrating successful reinforcement effects between the metallic silver and cellulosic fabric substrates. The discussions further confirmed the successful binding and deposition of green nanosilver on sisal/cotton interwoven fabrics.

Color and fastness studies of control and AgNP treated sisal/cotton interwoven fabrics. Color characteristics of control and nanosilver-coated sisal/cotton interwoven fabrics were also measured in order to investigate the effects of AgNPs on grey fabrics. Although the changes of color appearances in nanocolloids were observed visually, the colorful solid samples (nanosilver deposited) were assessed with the widely used spectrophotometric data, which is also considered a simple method to apply to colorimetric study. The investigated colorimetric data include K/S values and color coordinates (L^* , a^* , and b^*) as shown in Table 4. Therefore, the variation in color sensing capabilities were determined in terms of K/S and CIE (L^* , a^* , and b^*) values for all the test specimens. Table 4 clearly demonstrates that coloration using different treatments over sisal/cotton interwoven fabrics employing AgNO_3 has significant effects on perceived colors. The control fabric samples exhibited nearly white and lighter color tones (84.02) with very low K/S value (0.09) and with comparatively lower a^* (1.89) and b^* (6.8) values as well. The K/S values started to increase with the increase of AgNPs in the test samples. Test specimen 2 possessed only 2.74 K/S values, whereas sample 3 showed 6.76 and sample 4, a value of 8.96. In addition, it is further noticed that K/S values shown by EAg1 is 30.44, EAg2 by 75.11, and EAg3 by 100 times higher compared to control sample, which clearly confirmed that AgNP concentrations played a vital role regarding this changes. This clearly confirmed that AgNP concentrations played a vital role in these changes. Conversely, L^* values indicating the darkness/lightness values also exhibited a decreasing trend. The increase of silver contents by sample were as follows: from 84.02 for the control to 42.46, 29.74, and 25.95 for samples 2, 3, and 4, respectively. The Ag contents for the three samples were 16, 323, and 697 mg/L, respectively. As was the case with K/S values, increased Ag loading also made fabrics darker by as much 1.5, 1.7, and 1.87 times. In addition, the other values like a^* and b^* also showed positive integers, indicating the presence of reddish/yellowish tones in the color coordinates. Therefore, the colors displayed ranged from light orange (sample 2), to orange red (sample 3), and dark orange red (sample 4). Another reason for the color darkness was the increase of silver content formed more Ag^0 ; hence, the colors became darker due to LSPR effects. Finally, successful formations of colorful AgNPs were found on the surfaces of sisal/cotton interwoven fabrics. The perceived results achieved and discussed here are in agreement with other reports^{33,36}.

Statistical analysis of color characteristics. Initially, regression analysis for the coloration properties of all the samples were carried out in terms of nanosilver loading on sisal/cotton interwoven fabrics. Besides, the R^2 values as shown in Table 4 found for all the samples equal or higher than 0.95 demonstrating that the higher loading of AgNPs on fabric samples exist a positive attribution in terms of K/S, L^* , a^* , and b^* values. Furthermore, the perceived values in case of p are found to have less than 0.05 for all the coloration characteristics just except for the intercept in K/S value (marked through bold color), also indicate that there are significant effects of increased nanosilver loading on fabrics (Table 5, Table 6, Table 7, Table 8). Moreover, significance of the results was also further investigated by means of one-way ANOVA test where the samples were considered as

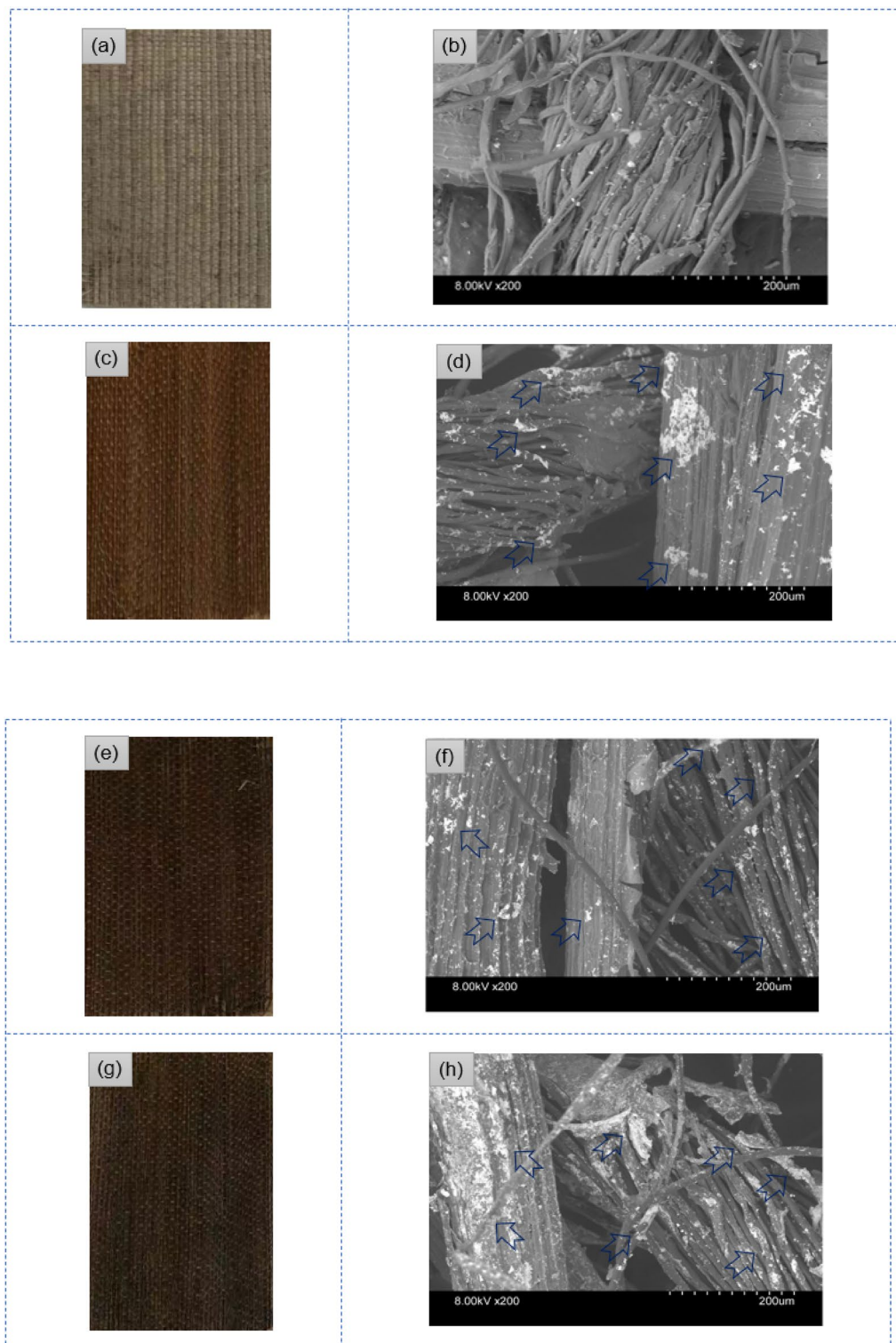


Figure 4. Physical photographs of control and nanosilver treated samples: (a) control sisal/cottons physical image, (b) control sisal/cottons morphological image, (c) physical image of EAg1, (d) morphological image of EAg1, (e) physical image of EAg2, (f) morphological image of EAg2, (g) physical image of EAg3, (h) morphological image of EAg3.

categorical factor. The associated F-tests also demonstrate the significance of all the coloration values. Moreover, pairwise comparison of different samples were also conducted by Fisher LSD test, reflecting a significant differ-

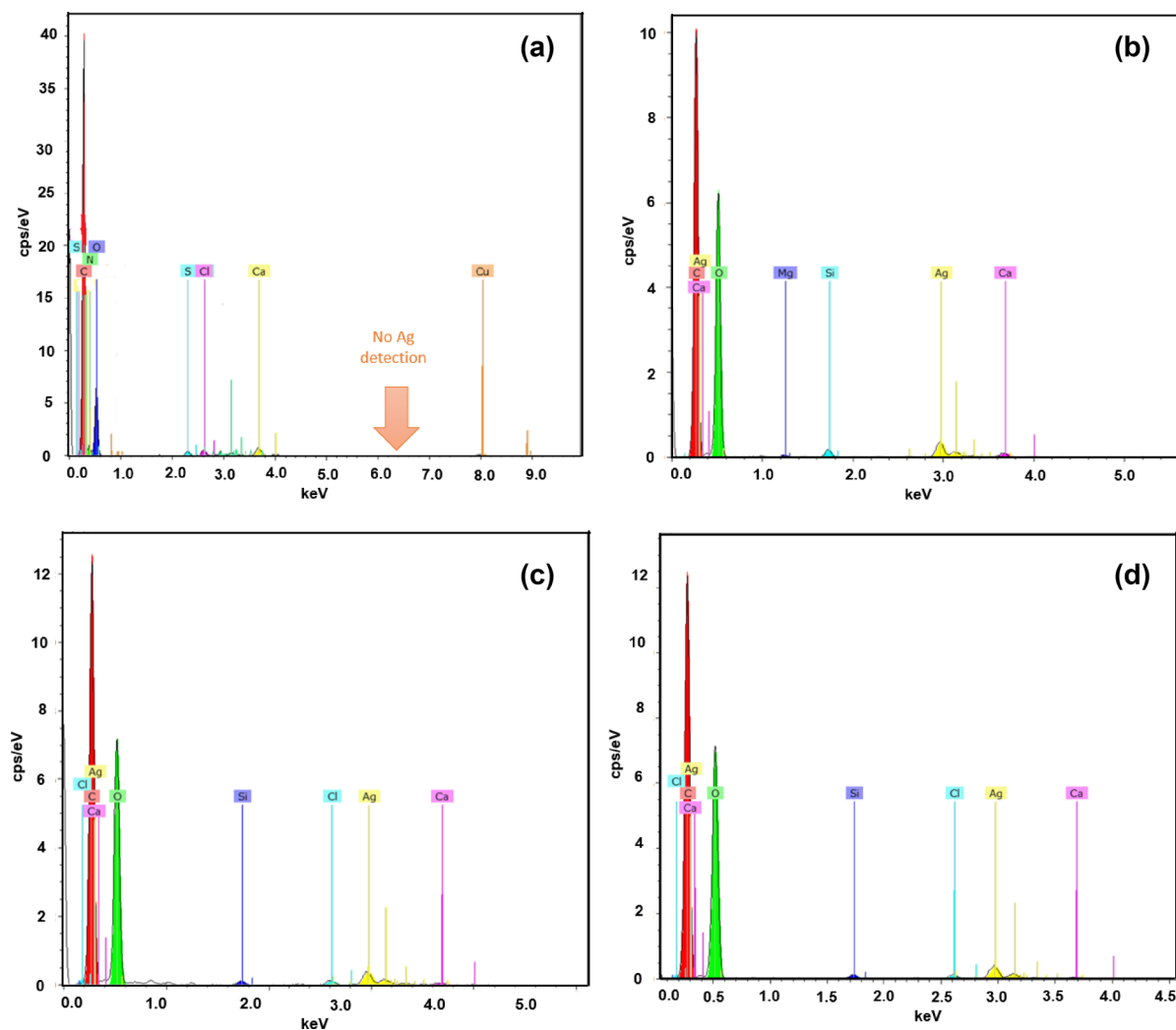


Figure 5. EDX spectra of the control and nanosilver treated sisal/cotton interwoven fabric specimens: (a) control sisal/cotton, (b) EAg1, (c) EAg2, and (d) EAg3.

Samples	Carbon (wt.%)	Oxygen (wt.%)	AgNP (wt.%)	Others (wt.%)
EAg0	50.08	47.94	–	<2.5
EAg1	41.37	45.6	9.462	<4
EAg2	43.39	44.1	9.463	<3.5
EAg3	43.3	43.1	9.95	<4

Table 3. Numerical values of EDX analysis for control and nanosilver-coated sisal/cotton interwoven fabrics.

ences within all the coloration values as the p value is less than 0.05 (assumed level) (Table 9, Table 10, Table 11, Table 12). However, a* value did not provide significant differences in two cases (Table 11) as marked through bold color. The similar effects of statistical analysis was reported in our previous study on flax/glass reinforced methylene diphenyl diisocyanate composite materials to understand the effects of glass in the system³⁷. Otherwise, the way we presented the statistical data in this current study is not available by other similar studies for understanding the influences of AgNPs in sisal/cotton interwoven fabrics.

The color characteristics are not restricted only to imparting color on fabrics, but also resist fading under certain conditions such as exposure to water and rubbing. Therefore, the durability of colors deposited on sisal/cotton fabrics was investigated in terms of washing and rubbing (both dry and wet conditions). The color durability of Sample 2 (lowest silver-containing fabric) was better with a higher loading of nanosilver. However, all the samples displayed better color stability. Sample 2, with a wash fastness value of 4, demonstrated “very good” color stability, whereas samples 3 and 4 had a rating of 3, indicating “good” color fastness to washing. On the other hand, samples 2 and 3 displayed a value of 3 for wet rubbing, which reflects “good” color durability. Sample 4 exhibited a value of 2, indicating “fair” fastness properties (Table 13). The trend in dry rubbing was nearly the

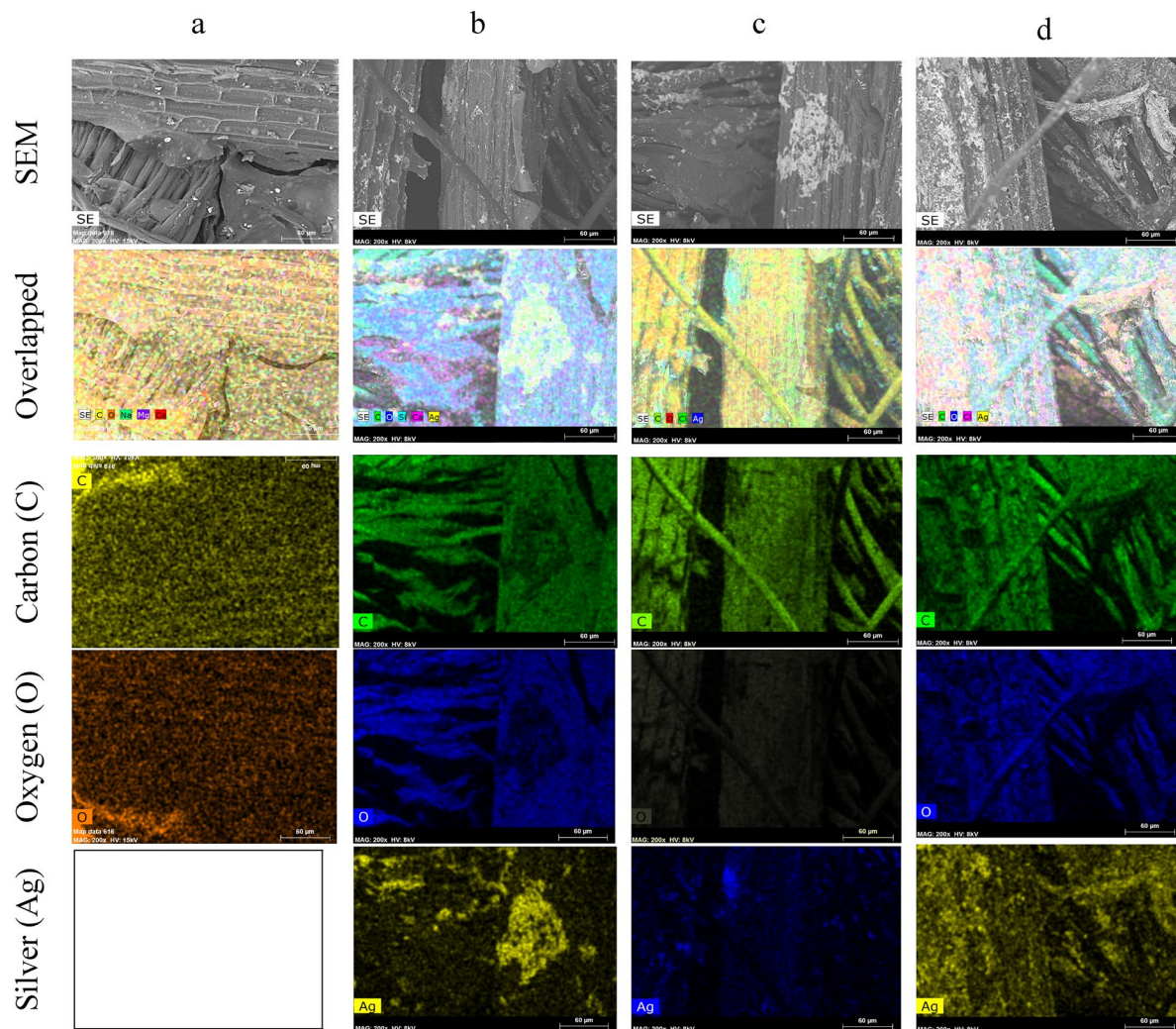


Figure 6. Elemental mapping images of control and AgNP treated sisal/cotton interwoven fabric specimens: EAg0 (a), EAg1 (b), and EAg2 (c), and (d) EAg3.

Samples	K/S	L*	a*	b*	Color evaluation
EAg0	0.09	84.02	1.89	6.8	Grey/nearly white
EAg1	2.74	42.46	12.98	38.64	Light orange
EAg2	6.76	29.74	16.84	47.56	Orange red
EAg3	8.96	25.95	17.19	43.19	Dark orange red
Coefficient of variations (R^2)	0.95	0.99	0.99	0.99	–

Table 4. Colorimetric data for control and nanosilver-coated sisal/cotton interwoven fabrics.

Effects	Parameter	Standard error	T	P
Intercept	0.600733	0.399822	1.50250	0.163871
Composition	0.163562	0.012322	13.27343	0.000000

Table 5. Regression analysis for K/S values in terms of nanosilver loading. Bold *p* values indicate not significant.

Effects	Parameter	Standard error	t	P
Intercept	68.64611	6.139479	11.18110	0.000001
Composition	-0.92900	0.189218	- 4.90968	0.000614

Table 6. Regression analysis for L* values in terms of nanosilver loading.

Effects	Parameter	Standard error	t	P
Intercept	6.210323	1.794346	3.461050	0.006112
Composition	0.247529	0.055302	4.475982	0.001186

Table 7. Regression analysis for a* values in terms of nanosilver loading.

Effects	Parameter	Standard error	t	P
Intercept	19.56498	5.305691	3.687546	0.004194
Composition	0.57852	0.163521	3.537891	0.005376

Table 8. Regression analysis for b* values in terms of nanosilver loading.

Samples	1	2	3	4
EAg0		0.003878	0.000011	0.000001
EAg1	0.003878		0.000507	0.000014
EAg2	0.000011	0.000507		0.005544
EAg3	0.000001	0.000014	0.005544	

Table 9. Fisher LSD test for K/S values in terms of different samples (nanosilver loading).

Samples	1	2	3	4
EAg0		0.000000	0.000000	0.000000
EAg1	0.000000		0.000002	0.000000
EAg2	0.000000	0.000002		0.002788
EAg3	0.000000	0.000000	0.002788	

Table 10. Fisher LSD test for L* values in terms of different samples (nanosilver loading).

Samples	1	2	3	4
EAg0		0.000000	0.000000	0.000000
EAg1	0.000000		0.000001	0.000002
EAg2	0.000000	0.000001		0.206463
EAg3	0.000000	0.000002	0.206463	

Table 11. Fisher LSD test for a* values in terms of different samples (nanosilver loading). Bold *p* values indicate not significant.

Samples	1	2	3	4
EAg0		0.000000	0.000000	0.000000
EAg1	0.000000		0.000064	0.006111
EAg2	0.000000	0.000064		0.004621
EAg3	0.000000	0.006111	0.004621	

Table 12. Fisher LSD test for b* values in terms of different samples (nanosilver loading).

Samples	Wash fastness	Description	Wet rubbing	Description	Dry rubbing	Description
EAg0	—		—		—	
EAg1	4	Very good	3	Moderate	3	Moderate
EAg2	3	Moderate	3	Moderate	2–3	Slightly fair
EAg3	3	Moderate	2	Fair	2	Fair

Table 13. Fastness characteristics for control and nanosilver-coated sisal/cotton interwoven fabrics.

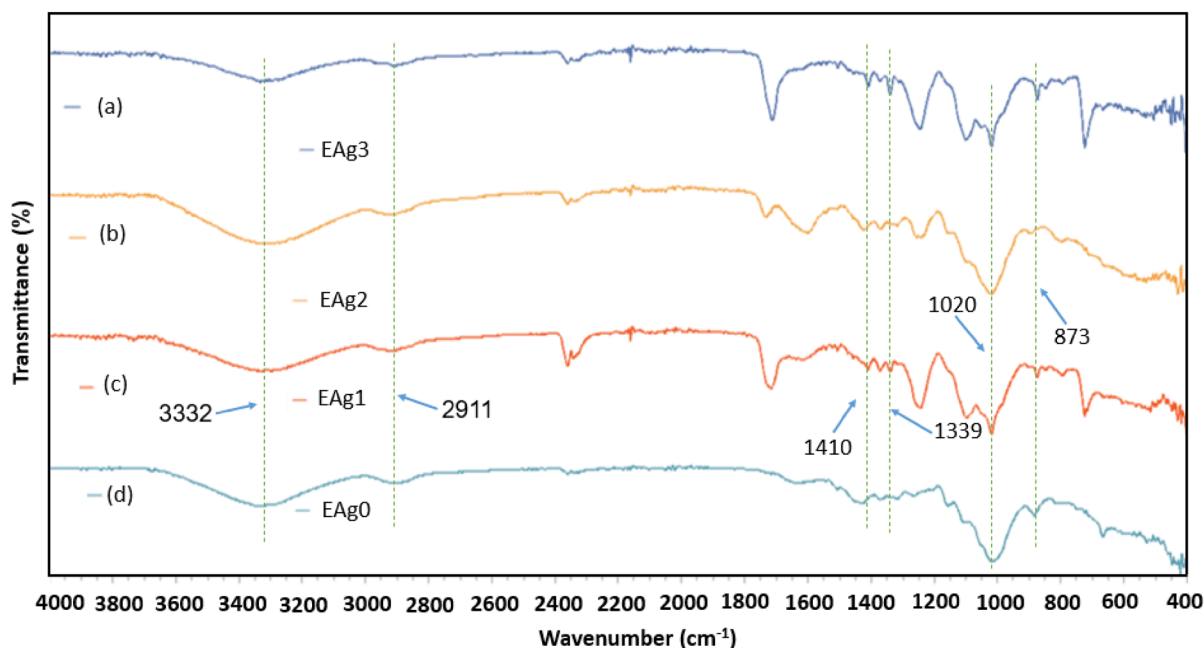


Figure 7. FTIR investigation of control and nanosilver-coated sisal/cotton interwoven fabrics.

same as the wet rubbing trend, which demonstrates “good” fastness characteristics, provides detailed data concerning the fastness of colorful nanosilver-coated sisal/cotton interwoven fabrics. The phenomenon found above also goes in agreement with some previous studies for AgNP colored textile substrates (natural fiber-based)^{38,39}.

FTIR investigations of control and nanosilver-coated sisal/cotton interwoven fabrics. The important characteristic bands of sisal/cotton interwoven fabrics and AgNP were explored using FTIR investigation (Fig. 7). Interestingly, no considerable shift was noticed before and after the nanosilver treatments on fabrics. The key characteristic bands of naturally derived sisal/cotton were found at 3332 cm^{-1} (—OH stretching), 2911 cm^{-1} (C—H stretching), and 1410 cm^{-1} (C—H wagging), 1339 cm^{-1} for C—H bending, 873 cm^{-1} (C—O stretching)^{40,41}. The peaks around 1714 cm^{-1} are related with the water absorbing molecules of cellulosic fibers⁴⁰. The bands around 1020 cm^{-1} are attributed to C—O—C stretching⁴². The treatment of sisal/cotton interwoven fabrics with nanosilver did not change the chemical structures of the fabrics as no new peaks appeared⁴³. In some cases, broad peaks appear after nanosilver treatment, which may be ascribed to the presence of European larch heartwood aqueous extracts in the system. However, the overall discussions demonstrate a successful bonding between the sisal/cotton interwoven fabrics and European larch heartwood mediated nanosilvers.

Thermal property investigations of control and nanosilver-coated sisal/cotton interwoven fabrics. Neat sisal/cotton interwoven fabrics and European larch heartwood mediated AgNPs were subjected for TGA and DTG analysis under nitrogen atmosphere. The thermogram photographs are displayed in Fig. 8. As with other cellulosic materials in which cellulose is the key chemical element, the degradation on weight in sisal/cotton interwoven fabrics started at 90 to 100 °C with moisture evaporation⁴⁴. The main weight loss occurred between 276 °C to 386 °C. This initial weight loss continued until 447 °C, demonstrating the degradation of cellulose⁴⁴. Another significant weight loss occurred at around 600 °C⁴⁴. The results confirm that European larch heartwood-mediated AgNP treatment slightly altered the thermal stability of sisal/interwoven fabrics when compared to the control, which concurs with the findings of a previous study⁴⁵. The peaks around 304 °C are associated with the hemicellulose degradations of sisal/cotton materials⁴⁶. Furthermore, the peaks around 364 °C for control sisal/cotton and around 375 °C for AgNP treated sisal/cotton indicate the cellulosic materials degradation from fibers⁴⁷. The phenomena discussed above clearly demonstrate the behavior of cellulosic compounds from naturally derived sisal/cotton materials at certain temperatures.

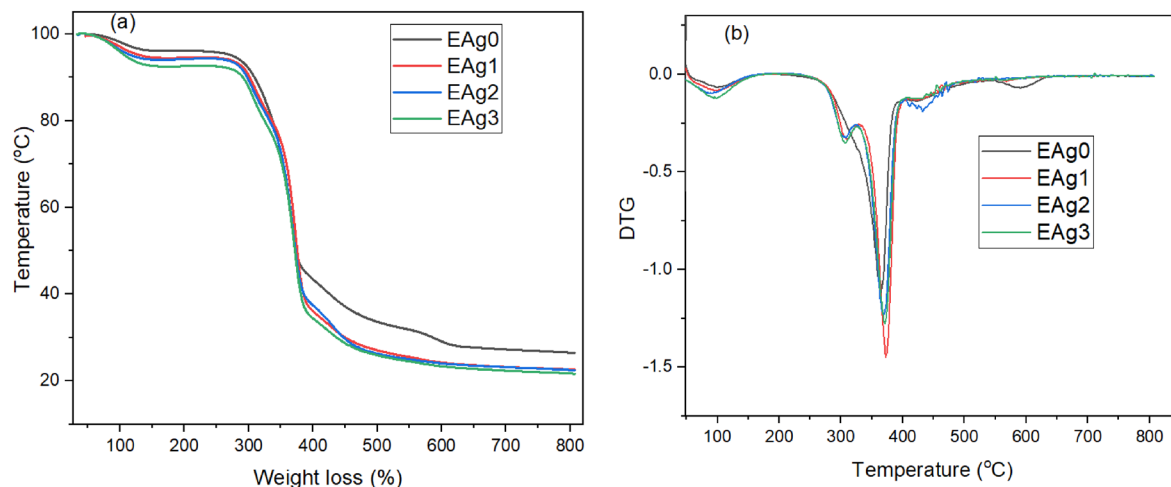


Figure 8. TGA and DTG analysis of control and nanosilver-coated sisal/cotton interwoven fabrics: (a) TGA and (b) DTG.

Conclusions

This study reported on the green synthesis of European larch heartwood mediated AgNPs deposited over sisal/cotton interwoven fabric with superior color characteristics and superior thermal stability. The key reason for the coloration is the LSPR properties of AgNPs in fabric surfaces during in situ synthesis protocol. The stated synthesis protocol and methodology is scalable, inexpensive, eco-friendly, and controllable. The formation of regulated AgNPs were confirmed by iCP OES analysis of aqueous solution, EDX, and elemental mapping of developed sustainable products. The quantified values of AgNPs present in aqueous solutions were 16 mg/L, 323 mg/L, and 697 mg/L for samples 2, 3, and 4, respectively. Moreover, morphological observations of the products also display strong and uniform distributions of AgNPs over the sisal/cotton fabric surfaces. The perceived K/S values of the nanosilver treated samples were 2.74, 6.76, and 8.96 for samples 2, 3, and 4, respectively. Conversely, the control sample provided a K/S value of only 0.09. The reported products also displayed significant thermal stability when exposed to heat. The current study has outlined a novel and facile route, one that has not yet been reported and could prove to be a milestone for the coloration industries, offering them a new solution with which to replace traditional colorants. The regression analysis and ANOVA test also confirmed further the significance of increased AgNPs loading on the fabric samples. The overall performance characteristics of the developed materials-sustainable sisal/cotton interwoven fabrics as well as colorful and thermally stable textiles-exhibited an eco-friendly and novel pathway that industry can utilize.

Received: 26 July 2021; Accepted: 13 October 2021

Published online: 17 November 2021

References

1. Talukder, M. E. *et al.* Novel fibrin functionalized multilayered electrospun nanofiber membrane for burn wound treatment. *J. Mater. Sci.* **56**, 12814–12834 (2021).
2. Kulkarni, N. & Muddapur, U. Biosynthesis of metal nanoparticles: a review. *J. Nanotechnol.* **2014**, 1–8. <https://doi.org/10.1155/2014/510246> (2014).
3. Barani, H., Boroumand, M. N. & Rafiei, S. Application of silver nanoparticles as an antibacterial mordant in wool natural dyeing: synthesis, antibacterial activity, and color characteristics. *Fibers Polym.* **18**, 658–665. <https://doi.org/10.1007/s12221-017-6473-8> (2017).
4. Hasan, K. E., Horváth, P. G., Horváth, A. & Alpár, T. Coloration of woven glass fabric using biosynthesized silver nanoparticles from *Fraxinus excelsior* tree flower. *Inorg. Chem. Commun.* **126**, 108477. <https://doi.org/10.1016/j.inoche.2021.108477> (2021).
5. Lai, C.-F. & Wang, Y.-C. Colloidal photonic crystals containing silver nanoparticles with tunable structural colors. *Curr. Comput.-Aided Drug Des.* **6**, 1–10. <https://doi.org/10.3390/cryst6050061> (2016).
6. Hasan, K. E., Wang, H., Mahmud, S. & Genyang, C. Coloration of aramid fabric via in-situ biosynthesis of silver nanoparticles with enhanced antibacterial effect. *Inorg. Chem. Commun.* **119**, 108115. <https://doi.org/10.1016/j.inoche.2020.108115> (2020).
7. Kuroiwa, Y. & Tatsuma, T. Laser printing of translucent plasmonic full-color images with transmission-scattering dichroism of silver nanoparticles. *ACS Appl. Nano Mater.* **3**, 2472–2479 (2020).
8. Molina, G. *et al.* Color and dichroism of silver-stained glasses. *J. Nanopart Res.* **15**, 1–13. <https://doi.org/10.1021/acsanm.9b02560> (2013).
9. Čuk, N., Šala, M. & Gorjanc, M. Development of antibacterial and UV protective cotton fabrics using plant food waste and alien invasive plant extracts as reducing agents for the in-situ synthesis of silver nanoparticles. *Cellulose* **28**, 3215–3233. <https://doi.org/10.1007/s10570-021-03715-y> (2021).
10. Mehata, M. S. Green synthesis of silver nanoparticles using *Kalanchoe pinnata* leaves (life plant) and their antibacterial and photocatalytic activities. *Chem. Phys. Lett.* **778**, 138760. <https://doi.org/10.1016/j.cplett.2021.138760> (2021).
11. Yu, Z. *et al.* Green synthesis of silver nanoparticles with black rice (*Oryza sativa* L.) extract endowing carboxymethyl chitosan modified cotton with high anti-microbial and durable properties. *Cellulose* **28**, 1827–1842. <https://doi.org/10.1007/s10570-020-03639-z> (2021).
12. Tavker, N. *et al.* Removal of cadmium and chromium by mixture of silver nanoparticles and nano-fibrillated cellulose isolated from waste peels of citrus sinensis. *Polymers* **13**, 234. <https://doi.org/10.3390/polym13020234> (2021).

13. Tang, B. *et al.* Coloration of cotton fibers with anisotropic silver nanoparticles. *Ind. Eng. Chem. Res.* **51**, 12807–12813. <https://doi.org/10.1021/ie3015704> (2012).
14. Yorseng, K., Rangappa, S. M., Pulikkalparambil, H., Siengchin, S. & Parameswaranpillai, J. Accelerated weathering studies of kenaf/sisal fiber fabric reinforced fully biobased hybrid bioepoxy composites for semi-structural applications: Morphology, thermo-mechanical, water absorption behavior and surface hydrophobicity. *Constr. Build. Mater.* **235**, 117464. <https://doi.org/10.1016/j.conbuildmat.2019.117464> (2020).
15. Ahith, D. *et al.* Effect of tungsten carbide on mechanical and tribological properties of jute/sisal/E-glass fabrics reinforced natural rubber/epoxy composites. *J. Ind. Text* **48**, 713–737 (2018).
16. Vieira, L. M. G. *et al.* Hybrid composites based on sisal fibers and silica nanoparticles. *Polym. Compos.* **39**, 146–156. <https://doi.org/10.1002/pc.23915> (2018).
17. Oliveira, F. R. *et al.* Photocatalytic properties of sisal fiber coated with nano titanium dioxide. *Mater. Today Proc.* **2**, 41–48. <https://doi.org/10.1016/j.matpr.2015.04.006> (2015).
18. Fakin, D., Veronovski, N., Ojstršek, A. & Božič, M. Synthesis of TiO₂-SiO₂ colloid and its performance in reactive dyeing of cotton fabrics. *Carbohydr. Polym.* **88**, 992–1001. <https://doi.org/10.1016/j.carbpol.2012.01.046> (2012).
19. Dhineshbabu, N., Arunmetha, S., Manivasakan, P., Karunakaran, G. & Rajendran, V. Enhanced functional properties of cotton fabrics using TiO₂/SiO₂ nanocomposites. *J. Ind. Text* **45**, 674–692 (2016).
20. Tudu, B. K., Sinhamahapatra, A. & Kumar, A. Surface modification of cotton fabric using TiO₂ nanoparticles for self-cleaning, oil–water separation, antistain, anti-water absorption, and antibacterial properties. *ACS Omega* **5**, 7850–7860. <https://doi.org/10.1021/acsomega.9b04067> (2020).
21. Hassabo, A. G., El-Naggar, M. E., Mohamed, A. L. & Hebeish, A. A. Development of multifunctional modified cotton fabric with tri-component nanoparticles of silver, copper and zinc oxide. *Carbohydr. Polym.* **210**, 144–156. <https://doi.org/10.1016/j.carbpol.2019.01.066> (2019).
22. Wu, M., Ma, B., Pan, T., Chen, S. & Sun, J. Silver-nanoparticle-colored cotton fabrics with tunable colors and durable antibacterial and self-healing superhydrophobic properties. *Adv. Funct. Mater.* **26**, 569–576. <https://doi.org/10.1002/adfm.201504197> (2016).
23. Vukoje, I. *et al.* The influence of triangular silver nanoplates on antimicrobial activity and color of cotton fabrics pretreated with chitosan. *J. Mater. Sci.* **49**, 4453–4460. <https://doi.org/10.1007/s10853-014-8142-2> (2014).
24. Ahmed, S., Ahmad, M., Swami, B. L. & Ikram, S. A review on plants extract mediated synthesis of silver nanoparticles for antimicrobial applications: a green expertise. *J. Adv. Res.* **7**, 17–28. <https://doi.org/10.1016/j.jare.2015.02.007> (2016).
25. Kanniah, P. *et al.* Green synthesis of multifaceted silver nanoparticles using the flower extract of *Aerva lanata* and evaluation of its biological and environmental applications. *Chem. Sel.* **5**, 2322–2331. <https://doi.org/10.1002/slct.201903228> (2020).
26. Gajendran, B. *et al.* Green synthesis of silver nanoparticle from *Datura innoxia* flower extract and its cytotoxic activity. *BioNanoScience* **9**, 564–572. <https://doi.org/10.1007/s12668-019-00645-9> (2019).
27. Oberhofnerová, E., Pánek, M., Podlena, M., Pavelek, M. & Štěrbová, I. Color stabilization of Siberian and European larch wood using UVA, HALS, and nanoparticle pretreatments. *Forests* **10**, 23. <https://doi.org/10.3390/f10010023> (2019).
28. Hasan, K., Horváth, P. G. & Alpár, T. Potential fabric-reinforced composites: a comprehensive review. *J. Mater. Sci.* <https://doi.org/10.1007/s10853-021-06177-6> (2021).
29. Gholampour, A. & Ozbakkaloglu, T. A review of natural fiber composites: properties, modification and processing techniques, characterization, applications. *J. Mater. Sci.* **55**, 829–892 (2020).
30. Hasan, K., Horváth, P. G. & Alpár, T. Potential natural fiber polymeric nanobiocomposites: a review. *Polymers* **12**, 1072. <https://doi.org/10.3390/polym12051072> (2020).
31. Eustis, S. & El-Sayed, M. A. Why gold nanoparticles are more precious than pretty gold: noble metal surface plasmon resonance and its enhancement of the radiative and nonradiative properties of nanocrystals of different shapes. *Chem. Soc. Rev.* **35**, 209–217. <https://doi.org/10.1039/B514191E> (2006).
32. Balamurugan, M., Saravanan, S. & Soga, T. Coating of green-synthesized silver nanoparticles on cotton fabric. *J. Coat. Technol. Res.* **14**, 735–745. <https://doi.org/10.1007/s10570-017-1204-2> (2017).
33. Ibrahim, H. M. & Hassan, M. S. Characterization and antimicrobial properties of cotton fabric loaded with green synthesized silver nanoparticles. *Carbohydr. Polym.* **151**, 841–850. <https://doi.org/10.1016/j.carbpol.2016.05.041> (2016).
34. Umoren, S. A., Nzila, A. M., Sankaran, S., Solomon, M. M. & Umoren, P. S. Green synthesis, characterization and antibacterial activities of silver nanoparticles from strawberry fruit extract. *Polish. J. Chem. Technol.* <https://doi.org/10.1515/pjct-2017-0079> (2017).
35. Colmenero-Flores, J. M. *et al.* Identification and functional characterization of cation–chloride cotransporters in plants. *Plant J.* **50**, 278–292. <https://doi.org/10.1111/j.1365-313X.2007.03048.x> (2007).
36. Kelly, F. M. & Johnston, J. H. Colored and functional silver nanoparticle–wool fiber composites. *ACS Appl. Mater. Int.* **3**, 1083–1092. <https://doi.org/10.1021/am101224v> (2011).
37. Hasan, K. F., Horváth, P. T. G. R. & Alpár, T. Thermomechanical behavior of methylene diphenyl diisocyanate-bonded flax/glass woven fabric reinforced laminated composites. *ACS Omega* **6**, 6124–6133. <https://doi.org/10.1680/jgrma.20.00052> (2021).
38. Hasan, K. F. *et al.* Coloration of flax woven fabric using *Taxus baccata* heartwood extract mediated nanosilver. *Colour Technol.* **00**, 1–11. <https://doi.org/10.1111/cote.12578> (2021).
39. Mia, R. *et al.* Functionalizing cotton fabrics through herbally synthesized nanosilver. *Clean Eng. Technol.* **4**, 100227. <https://doi.org/10.1016/j.clet.2021.100227> (2021).
40. Ahmed, H., Khattab, T. A., Mashaly, H., El-Halwagy, A. & Rehan, M. Plasma activation toward multi-stimuli responsive cotton fabric via in situ development of polyaniline derivatives and silver nanoparticles. *Cellulose* **27**, 2913–2926. <https://doi.org/10.1007/s10570-020-02980-7> (2020).
41. Chung, C., Lee, M. & Choe, E. K. Characterization of cotton fabric scouring by FT-IR ATR spectroscopy. *Carbohydr. Polym.* **58**, 417–420. <https://doi.org/10.1016/j.carbpol.2004.08.005> (2004).
42. Rehan, M., Abdel-Wahed, N. A., Farouk, A. & El-Zawahry, M. M. Extraction of valuable compounds from orange peel waste for advanced functionalization of cellulosic surfaces. *ACS Sustain. Chem. Eng.* **6**, 5911–5928. <https://doi.org/10.1021/acssuschemeng.7b04302> (2018).
43. Tang, B., Kaur, J., Sun, L. & Wang, X. Multifunctionalization of cotton through in situ green synthesis of silver nanoparticles. *Cel-lulose* **20**, 3053–3065. <https://doi.org/10.1007/s10570-013-0027-z> (2013).
44. Butola, B. & Verma, D. Facile synthesis of chitosan–silver nanoparticles onto linen for antibacterial activity and free-radical scavenging textiles. *Int. J. Boil. Macromol.* **133**, 1134–1141. <https://doi.org/10.1016/j.ijbiomac.2019.04.186> (2019).
45. Gollapudi, V. R. *et al.* In situ generation of silver and silver oxide nanoparticles on cotton fabrics using *Tinospora cordifolia* as bio-reductant. *SN Appl. Sci.* **2**, 1–10. <https://doi.org/10.1007/s42452-020-2331-1> (2020).
46. Hasan, K. F., Horváth, P. G., Kóczán, Z. & Alpár, T. Thermo-mechanical properties of pretreated coir fiber and fibrous chips reinforced multilayered composites. *Sci. Rep.* **11**, 1–13. <https://doi.org/10.1038/s41598-021-83140-0> (2021).
47. Hasan, K. M. F., Péter, G. H., Kóczán, Z. & Tibor, A. Thermo-mechanical properties of pretreated coir fiber and fibrous chips reinforced multilayered composites. *Sci. Rep.* <https://doi.org/10.1038/s41598-021-83140-0> (2021).

Acknowledgements

This work was funded and supported by the “Stipendium Hungaricum” scholarship under the Simonyi Károly Faculty of Engineering, Wood Sciences, and Applied Arts, University of Sopron, Hungary. This article was produced within the framework of “EFOP-3.6.1-16-2016-00018: improving the role of research, development and innovation in the higher education through institutional developments assisting intelligent specialization in Sopron and Szombathely”. Authors are highly grateful to Pro Horto Ltd. company for their cordial support to conduct this research.

Author contributions

K.M.F.H. generated the idea, conducted the experiment, performed the data curation, and wrote the initial draft. M.B. and Z.K. cooperated in data curation and investigation. P.G.H. and T.A. helped in project administration, data validation, and final draft review.

Competing interests

The authors declare no competing interests.

Additional information

Correspondence and requests for materials should be addressed to K.H. or T.A.

Reprints and permissions information is available at www.nature.com/reprints.

Publisher’s note Springer Nature remains neutral with regard to jurisdictional claims in published maps and institutional affiliations.



Open Access This article is licensed under a Creative Commons Attribution 4.0 International License, which permits use, sharing, adaptation, distribution and reproduction in any medium or format, as long as you give appropriate credit to the original author(s) and the source, provide a link to the Creative Commons licence, and indicate if changes were made. The images or other third party material in this article are included in the article’s Creative Commons licence, unless indicated otherwise in a credit line to the material. If material is not included in the article’s Creative Commons licence and your intended use is not permitted by statutory regulation or exceeds the permitted use, you will need to obtain permission directly from the copyright holder. To view a copy of this licence, visit <http://creativecommons.org/licenses/by/4.0/>.

© The Author(s) 2021